

Supporting Information

Defective Graphitic Carbon Nitride Synthesized by Controllable Co-polymerization with Enhanced Visible Light Photocatalytic Hydrogen Evolution

Mei Zhang,^{a,b} Yanyan Duan,^b Hanzhong Jia,^b Fu Wang,^{*b} Lan Wang,^b Zhi Su,^{*a} and Chuanyi Wang^{*b}

^a *College of Chemistry and Chemical Engineering, Xinjiang Normal University, Urumqi, Xinjiang 830054, China*

^b *Laboratory of Environmental Sciences and Technology, Xinjiang Technical Institute of Physics & Chemistry, Key Laboratory of Functional Materials and Devices for Special Environments, Chinese Academy of Sciences, Urumqi, Xinjiang 830011, China*

E-mail: suzhixj@sina.com, wangfu@ms.xjb.ac.cn, cywang@ms.xjb.ac.cn

*Corresponding author, Fax: +86-991-4332683. Tel: +86-991-4332683.

Table S1. Elemental composition of g-C₃N₄, CN-DT, CN-DMT, and CN-DPT

| Samples | N (%) | C (%) | H (%) | C/N (mass ratio) |
|---------------------------------|-------|-------|-------|---------------------|
| g-C ₃ N ₄ | 59.21 | 32.42 | 1.89 | 0.547 |
| CN-DT 1-10 | 58.18 | 31.96 | 1.84 | 0.549 |
| CN-DMT 1-10 | 58.20 | 32.82 | 1.84 | 0.564 |
| CN-DPT 1-10 | 60.47 | 35.70 | 1.76 | 0.590 |

Table S2. Elemental composition of CN-DPT with different amounts of DPT

| Samples | N% | C% | H% | DPT/Melamine (mass ratio) | Final C/N (mass ratio) |
|-------------|-------|-------|------|------------------------------|---------------------------|
| CN-DPT 1-05 | 59.26 | 35.82 | 1.76 | 0.200 | 0.604 |
| CN-DPT 1-10 | 60.47 | 35.70 | 1.76 | 0.100 | 0.590 |
| CN-DPT 1-15 | 60.54 | 35.48 | 1.76 | 0.067 | 0.586 |
| CN-DPT 1-20 | 60.83 | 35.37 | 1.78 | 0.050 | 0.581 |

S1. FT-IR Spectra of g-C₃N₄, CN-DT, CN-DMT, and CN-DPT

Figure S1 displays FTIR spectra of g-C₃N₄, CN-DT, CN-DMT and CN-DPT. The distinct peaks of g-C₃N₄ and modified g-C₃N₄ are located in the region of 1200-1600 cm⁻¹, which can be attributed to the stretching vibration of aromatic C-N heterocycle. The sharp peak at 805 cm⁻¹ is ascribed to the breathing mode of tri-s-triazine units, which further proves that incorporation of these functional monomers does not alter the skeleton of g-C₃N₄.¹

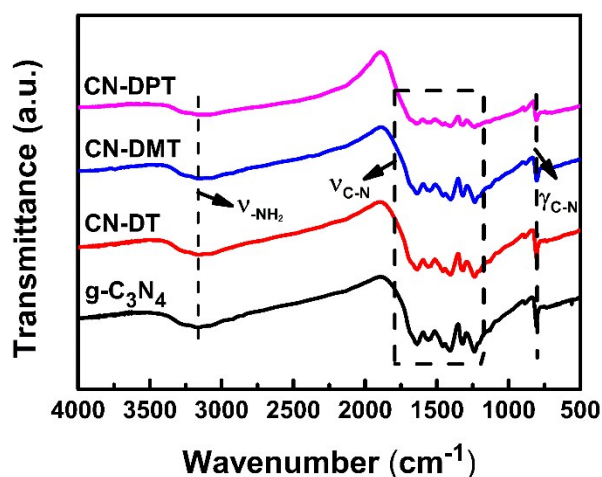


Figure S1. FT-IR spectra of $g\text{-C}_3\text{N}_4$, CN-DT, CN-DMT, and CN-DPT.

S2. Raman Spectra of $g\text{-C}_3\text{N}_4$, CN-DPT, and CN-CDT

Raman spectra were carried out to study the microstructure evolution of the $g\text{-C}_3\text{N}_4$, CN-DT, CN-DMT, and CN-DPT. The normalized Raman spectra of all samples are shown in Figure S2, several characteristic peaks of $g\text{-C}_3\text{N}_4$ at 705, 987, 1238 cm^{-1} is observed, which is consistent with the literature. Both 705 and 987 cm^{-1} peaks are corresponded to the breathing modes of triazine ring,²⁻⁵ and the peak at 1238 cm^{-1} is assigned to the $=\text{C}$ (sp^2) bending vibration.⁶ When comparing the Raman spectra of the pristine $g\text{-C}_3\text{N}_4$ with modified $g\text{-C}_3\text{N}_4$, two obvious spectral features are noticed. The first one is that CN-DT and CN-DMT show nearly identical Raman shifts of $g\text{-C}_3\text{N}_4$, suggesting CN-DT or CN-DMT retain the similar structure with $g\text{-C}_3\text{N}_4$. The second feature is that CN-DPT appears a new broad peak at 839 cm^{-1} , which might result from the incorporation of aromatic organic molecules into the carbon nitride network. Besides that, we also use CDT as a monomer to modify the carbon nitride, which has one more phenyl group than DPT. It is clear that the Raman spectra of CN-CDT and $g\text{-C}_3\text{N}_4$ are completely different. Therefore, we deduce that introduce excessive large groups in CN-CDT samples will affect the copolymerization and destroy the integrated structure of carbon nitride. It is worth pointing out that the inconspicuous of some of the Raman structural peaks and the appearance of many noise peaks is due to the weak Raman

signal of $g\text{-C}_3\text{N}_4$ and strong fluorescent background.

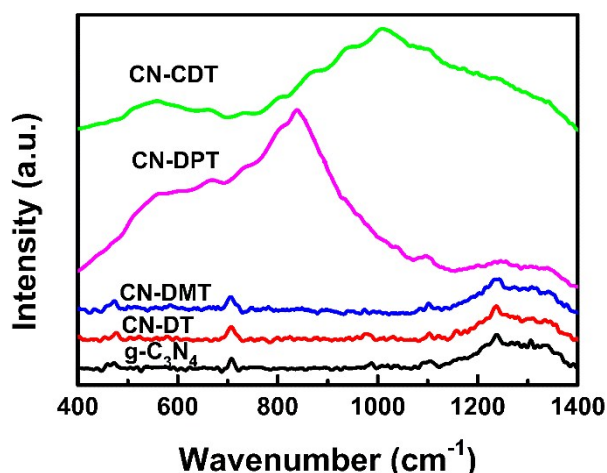


Figure S2. Raman spectra of $g\text{-C}_3\text{N}_4$, CN-DT, CN-DMT, CN-DPT, and CN-CDT excited with a 785 nm laser.

S3. SEM Images of $g\text{-C}_3\text{N}_4$, CN-DT, CN-DMT, CN-DPT, and CN-CDT

Figure S3 exhibits the morphologies of the obtained samples. As shown in Figure S3a, the pristine $g\text{-C}_3\text{N}_4$ displays bulk morphology in a micrometer scale, which is in agreement with the TEM observation. In comparison, the modified $g\text{-C}_3\text{N}_4$ possess more and larger pores with the increase of terminal functional groups (Figure S3b-d). The change of morphology might be ascribed to the lack of reactive sites. Monomers with two phenyl groups are also applied to synthesize $g\text{-C}_3\text{N}_4$, the morphology of as-prepared sample is displayed in Figures S3e and S3f. It can be seen that small particles disperse in the agglomerates structure, suggesting that introduce excessive larger groups will affect the copolymerization and destroy the π -conjugation structure in $g\text{-C}_3\text{N}_4$.

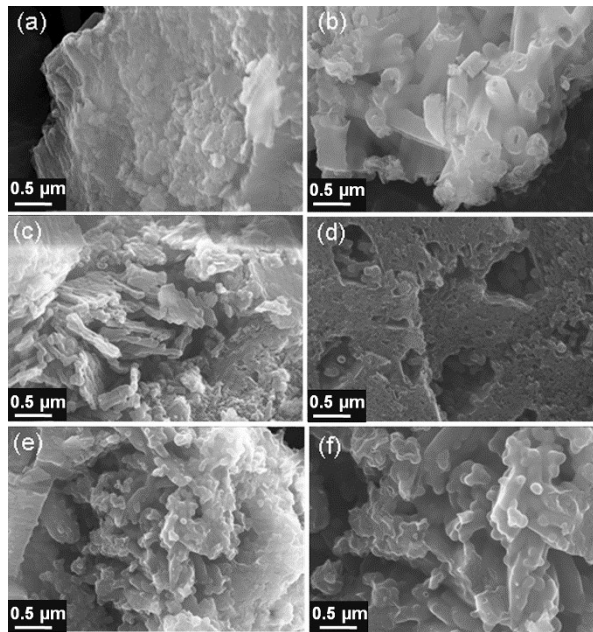


Figure S3. SEM images of g-C₃N₄ (a), CN-DT (b), CN-DMT (c), CN-DPT (d), and CN-CDT (e), (f).

S4. Valence Band (VB) XPS Spectra of g-C₃N₄, CN-DT, CN-DMT, and CN-DPT

Figure S4 shows the VB XPS spectra of g-C₃N₄, CN-DT, CN-DMT, and CN-DPT. Compared with the spectrum of g-C₃N₄, a negative shift is observed in the modified g-C₃N₄ spectrum. The VB potentials of CN-DT, CN-DMT, and CN-DPT are located at 1.83, 1.73, and 1.62 eV, respectively.

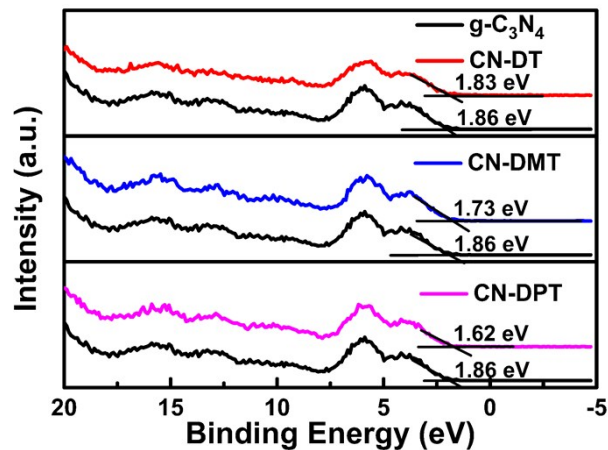


Figure S4. XPS valence band spectra of g-C₃N₄, CN-DT, CN-DMT, and CN-DPT.

S5. PL Spectra of g-C₃N₄, CN-DT, CN-DMT, and CN-DPT

As shown in Figure S5, the PL emission spectra were performed to inspect the separation of the photo-generated carriers in pristine and modified g-C₃N₄. The PL intensity of the CN-DPT is obviously reduced in comparison with pristine g-C₃N₄ (the absorption of samples is kept

approximately equal at 315 nm), which indicates a lower recombination rate of photogenerated electrons and holes.^{7,8}

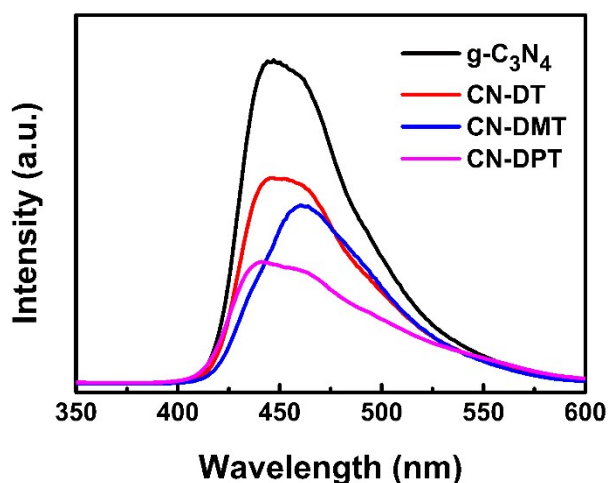


Figure S5. PL spectra of pristine $g\text{-C}_3\text{N}_4$ and modified $g\text{-C}_3\text{N}_4$ under 315 nm excitation.

S6. Hydrogen Production of CN-DT_x , CN-DMT_x , and CN-DPT_x

As shown in Figure S6, we have studied the effects of different ratio on the photocatalytic activities of these monomers. The results demonstrate that the hydrogen production of all modified $g\text{-C}_3\text{N}_4$ show consecutive increase from -H to $-\text{C}_6\text{H}_6$. Moreover, when the proportion of these monomers to melamine is at 1 to 10, the modified $g\text{-C}_3\text{N}_4$ (CN-DT, CN-DMT, and CN-DPT) show the best photocatalytic activities.

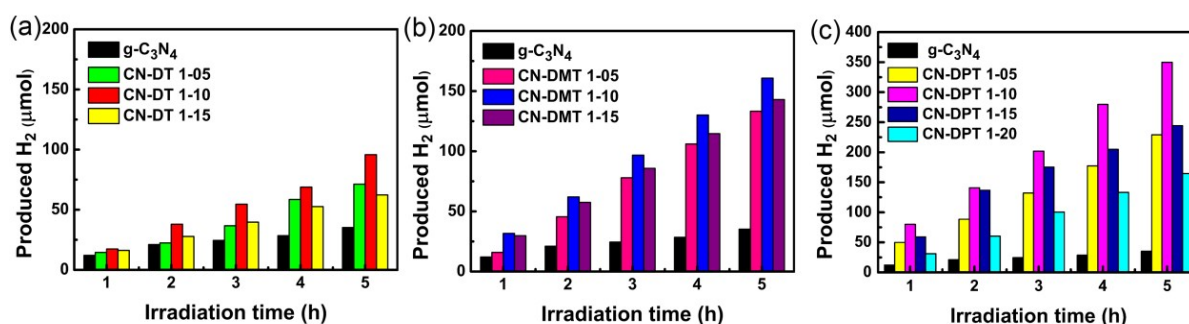


Figure S6. Time-dependent hydrogen evolution in different amounts of CN-DT_x (a), CN-DMT_x (b), CN-DPT_x (c), and pristine $g\text{-C}_3\text{N}_4$ under visible light irradiation ($\lambda \geq 420$ nm).

S7. XRD Patterns of $g\text{-C}_3\text{N}_4$ and CN-CDT

XRD patterns of pristine $g\text{-C}_3\text{N}_4$ and CN-CDT are shown in Figure S7. There is no obvious

distinction between the patterns of CN-CDT and $g\text{-C}_3\text{N}_4$, confirming CN-CDT maintains the structure of triazine. Comparing with $g\text{-C}_3\text{N}_4$, the dominant (002) peak of CN-CDT shifts to lower angle which might stem from the increase of the interplanar distance of CN-CDT, suggesting that incorporated CDT can introduce disorders in the layered structure.

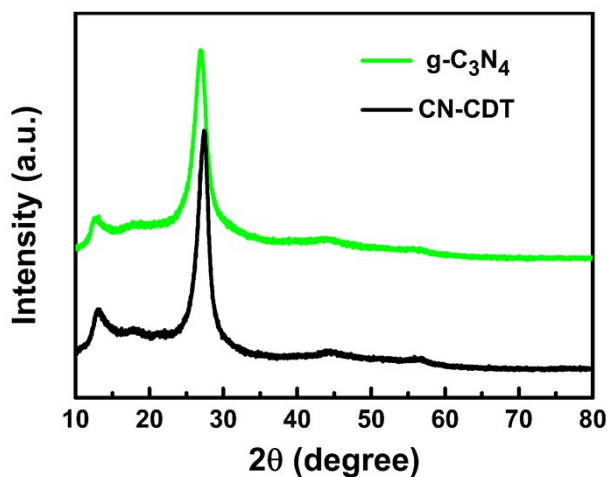


Figure S7. XRD patterns of pristine $g\text{-C}_3\text{N}_4$ and CN-CDT.

S8. N_2 Sorption Isotherms of $g\text{-C}_3\text{N}_4$ and CN-CDT

Figure S8 shows the N_2 sorption isotherms of $g\text{-C}_3\text{N}_4$ and CN-CDT. When the number of functional groups increases to two, the S_{BET} value drop severely, which further convinces that two phenyl will destroy the π -conjugation in $g\text{-C}_3\text{N}_4$ structure.⁹

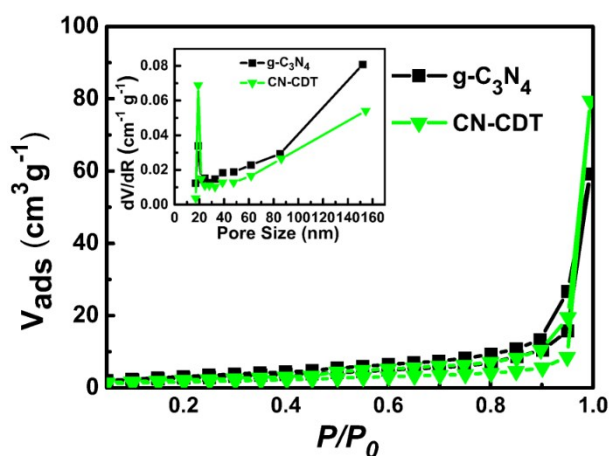


Figure S8. N_2 sorption isotherms of $g\text{-C}_3\text{N}_4$ and CN-CDT; inset Figure illustrates the pore size distribution.

S9. EPR Spectra of g-C₃N₄, CN-DPT, and CN-CDT

Figure S9 shows the EPR spectra of g-C₃N₄, CN-DPT, and CN-CDT in the dark. It is clear that the EPR signal of CN-CDT is relatively weaker than CN-DPT, which might stem from the destroyed conjugation structure.

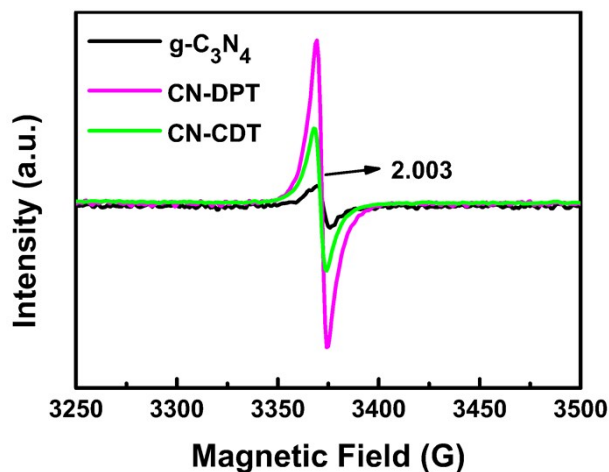


Figure 9. EPR spectra of g-C₃N₄, CN-DPT, and CN-CDT under dark.

Reference

- 1 Y. Cui, G. Zhang, Z. Lin and X. Wang, *Appl. Catal. B*, 2016, **181**, 413-419.
- 2 Q. Xiang, J. Yu and M. Jaroniec, *J. Phy. Chem. C*, 2011, **115**, 7355-7363.
- 3 X. Zhang, X. Xie, H. Wang, J. Zhang, B. Pan and Y. Xie, *J. Am. Chem. Soc.*, 2013, **135**, 18-21.
- 4 Y. Shiraishi, S. Kanazawa, Y. Sugano, D. Tsukamoto, H. Sakamoto and T. Hirai, *ACS Catal.*, 2014, **4**, 774-780.
- 5 P. V. Zinin, L. C. Ming, S. K. Sharma, V. N.Khabashesku, X. Liu, S. Hong and T. Acosta, *Chem. Phy. Lett.*, 2009, **472**, 69-73.
- 6 J. Jiang, L. Yang, L. Zhu, A. Zheng, J. Zou, X. Yi and H. Tang, *Carbon*, 2014, **80**, 213-221.
- 7 Y. P. Zhu, T. Z. Ren and Z. Y. Yuan, *ACS Appl. Mater. Interfaces*, 2015, **7**, 16850-16856.
- 8 J. Zhang, M. Zhang, G. Zhang and X. Wang, *ACS Catal.*, 2012, **2**, 940-948.
- 9 W. Ho, Z. Zhang, W. Lin, S. Huang, X. Zhang, X. Wang and Y. Huang, *ACS Appl. Mater. Interfaces*, 2015, **7**, 5497-5505.